

Transmission Capacity of Full-Duplex MIMO Ad-Hoc Network with Limited Self-Interference Cancellation

Jiancao Hou and Mohammad Shikh-Bahaei

Centre for Telecommunications Research, King's College London, London, UK

e-mail: {jiancao.hou, m.sbahaei}@kcl.ac.uk

Abstract—In this paper, we propose a joint transceiver beamforming design to mitigate self-interference and inter-node interference simultaneously for full-duplex multiple-input and multiple-output ad-hoc network, and derive the transmission capacity upper bound (TC-UB) for the considered network. Condition on a specified transceiver antenna's configuration, we allow the self-interference effect to be cancelled at transmitter side, and offer an additional degree-of-freedom at receiver side for more inter-node interference cancellation. In addition, due to the imperfect self-interference channel estimation, the derivation of TC-UB needs to take the channel estimation error into account. In this case, the conventional method to obtain the TC-UB is not applicable. This motivates us to exploit the dominating interferer region and then utilize Newton-Raphson method to iteratively formulate the TC-UB. The results show that the derived TC-UB is quite close to the actual one especially when the number of receive-antenna is small. Moreover, our proposed beamforming design outperforms the existing beamforming strategies.

I. INTRODUCTION

Due to the rapid expansion of applications and services, next generation wireless networks are expected to rely on low latency and high spectral efficiency [1]–[4]. In-band full-duplex (IBFD) as one of promising techniques has recently re-emerged to achieve such requirements [5]–[8]. Unlike the conventional half-duplex (HD) radio transceiver design, IBFD is able to transmit and receive simultaneously over the same spectrum. In theory, it can halve latency and double spectral efficiency of point-to-point communications if the self-interference (SI) effect can be cancelled perfectly. On the other hand, many researchers have contributed to develop advanced techniques to handle the SI effect, such as propagation-domain antenna separation [9], [10], analog-domain and/or digital-domain SI cancellation [11]–[13]. Although these techniques can potentially yield impressive SI cancellation, their performances degrade considerably if the SI channel state information (CSI) is not modelled/estimated accurately.

Consider a FD ad-hoc wireless network, where multiple transceiver pairs communicate simultaneously without central control unit. The SI and the inter-node interference as the significant barriers limit the rate of successful transmissions. Employing efficiently radio resource allocation methods as in [14]–[16], or multiple-input and multiple-output (MIMO) techniques as in [17], [18] can well manage these interferences and improve the successful transmissions with high

data rate. Transmission capacity (TC), which characterizes the maximum node density of successful transmissions of a network, has been investigated intensively for some specific HD MIMO strategies in [19]–[21]. Since there is no SI presented, the performance analysis in terms of TC can be easily conducted by exploiting the statistical property of the accumulated inter-node interference via 1-D Poisson point process (PPP). Considering FD with multiple antennas at each node, the SI has attracted many research efforts to cancel it in spatial domain [22]–[24]. In addition, the performance analysis on the network have been investigated in [25]–[27], where the authors provided the throughput/achievable sum-rate analysis at present of residual SI and/or some inter-node interference cancellation strategies. To the best of our knowledge, the theoretical analysis of TC for FD MIMO ad-hoc network at present of SI channel estimation error has not been well studied, where the analysed TC framework gives a simple expression for quantification of achievable rate.

Motivated by the above discussion, in this paper, we first propose a joint transceiver beamforming design to mitigate inter-node interference and SI effects for the FD MIMO ad-hoc network. In this case, by exploiting a specific transceiver antenna's configuration, partial SI can be cancelled at transmitter side and leave an additional degree-of-freedom (DoF) at receiver side for more inter-node interference cancellation. Then, we derive the TC upper bound (TC-UB) of considered model at present of SI channel estimation error.¹ Unlike the TC-UB derivation in HD case [19]–[21], the TC-UB derivation in FD case cannot resort to the standard 1-D PPP to get the expected distance of dominating interferer from the typical receiver. Thus, we exploit the dominating interferer region with generalized 2-D PPP and then utilize Newton-Raphson method to iteratively formulate the TC-UB. The results show that the derived TC-UB is quite close to the simulated curve especially with large transmit-antenna to receive-antenna ratio (TRR). Moreover, our proposed transceiver beamforming design outperforms the existing beamforming strategies, e.g., singular value decomposition (SVD) and partial zero-forcing (ZF) methods. Finally, we compare our derived TC-UB of FD

¹The reason we did not consider the TC lower bound is because it only works in certain conditions and can be easily obtained by extending the analytical work in [28].

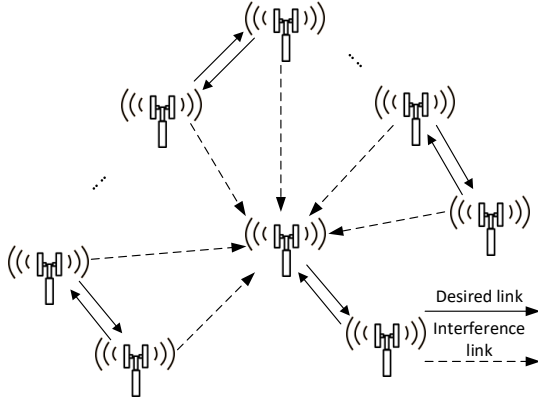


Fig. 1: An example of full duplex ad-hoc network.

case with the ones of HD case, and highlight the importance of dominating inter-node interference cancellation.

II. SYSTEM MODEL

Consider an interference-limited ad-hoc network as shown in Fig.1, where each node has FD capability and is equipped with N antennas. N_t is the number of transmit-antenna and $N_r (= N - N_t)$ is the number of receive-antenna. The nodes in the network are divided into two different sets, e.g., $\Phi_A = \{a_k, k=0,1,\dots,M-1\}$ and $\Phi_B = \{b_k, k=0,1,\dots,M-1\}$, where the nodes locations of each set follows a stationary PPP with intensity λ . In addition, node a_k in Φ_A is paired with node b_k in Φ_B , $k = 0, 1, \dots, M-1$. To simplify the analysis, the distance of each transceiver pair is fixed to L , and the transmission power of each node is set to P . We also assume each node can perfectly estimate its associated links' CSI except the SI channel.

We select a node pair, e.g., $\{a_0, b_0\}$, as the typical link pair. According to Slivnyak's theorem [29], the properties of node $a_0 \in \Phi_A$ (or node $b_0 \in \Phi_B$) represent the properties of other nodes in the same set. In addition, due to FD capability, node a_0 receives interferences not only from Φ_A/a_0 but also from Φ_B/b_0 . Accordingly, the received signal at node $i \neq j \in \{a_0, b_0\}$ with size of $N_r \times 1$ can be expressed as

$$\mathbf{y}_i = \sqrt{P}L^{-\alpha/2}\mathbf{H}_{i,j}\mathbf{x}_j + \sqrt{P}\sum_{k=1}^{M-1}r_{b_k}^{-\alpha/2}\mathbf{H}_{i,b_k}\mathbf{x}_{b_k} + \sqrt{P}\sum_{k=1}^{M-1}r_{a_k}^{-\alpha/2}\mathbf{H}_{i,a_k}\mathbf{x}_{a_k} + \sqrt{P}\mathbf{H}_i\mathbf{x}_i + \mathbf{v}_i, \quad (1)$$

where \mathbf{x}_{b_k} and \mathbf{x}_{a_k} with size of $N_t \times 1$ are the transmitted signal from node b_k and node a_k , respectively; \mathbf{H}_{i,b_k} and \mathbf{H}_{i,a_k} with size of $N_r \times N_t$ denote channel fading effects from node b_k to node i and from node a_k to node i , respectively, and they are independent and identically distributed (i.i.d.) complex Gaussian random variables with zero mean and unit variance per element. r_{b_k} and r_{a_k} represent the distances from node b_k to node i and from node a_k to node i , respectively. $\alpha > 2$ is the path-loss exponent. \mathbf{v}_i with size of $N_r \times 1$ denotes

the additive white Gaussian noise (AWGN) at node i with zero mean and unit variance. Moreover, due to imperfect SI channel estimation, we have

$$\mathbf{H}_i = \hat{\mathbf{H}}_i + \mathbf{\Delta}_i, \quad (2)$$

where \mathbf{H}_i is the actual self-interference channel, $\hat{\mathbf{H}}_i$ is its estimated version, and $\mathbf{\Delta}_i$ is the estimation error following complex Gaussian distribution with zero mean and $\sigma_{i,\text{SI}}^2$ variance per element. Here, we assume $\hat{\mathbf{H}}_i$ and the statistical information of $\mathbf{\Delta}_i$ are known by node i .

With the local CSIs at each node, we can formulate the pre-processing/post-processing beamforming vectors to mitigate the SI and the inter-node interference. Specifically, let's denote $\mathbf{w}_{b_k} \in \mathcal{C}^{N_t \times 1}$ and $\mathbf{w}_{a_k} \in \mathcal{C}^{N_t \times 1}$ as the pre-processing beamforming vectors for node b_k and node a_k , respectively. Then, we have the transmitted signals

$$\mathbf{x}_{b_k} = \mathbf{w}_{b_k} s_{b_k}, \quad k = 0, 1, \dots, M-1, \quad (3)$$

$$\mathbf{x}_{a_k} = \mathbf{w}_{a_k} s_{a_k}, \quad k = 0, 1, \dots, M-1, \quad (4)$$

where s_{b_k} and s_{a_k} represent the data symbols at node b_k and node a_k , respectively, and the power of \mathbf{x}_{b_k} and \mathbf{x}_{a_k} are normalized to one. Subsequently, the received signal at the typical node $i \neq j \in \{a_0, b_0\}$, after applying the post-processing beamforming vector \mathbf{z}_i , can be expressed as

$$\mathbf{z}_i^H \mathbf{y}_i = \sqrt{P}L^{-\alpha/2}h_{i,j} + \sqrt{P}\sum_{k=1}^{M-1}r_{b_k}^{-\alpha/2}h_{i,b_k} + \sqrt{P}\sum_{k=1}^{M-1}r_{a_k}^{-\alpha/2}h_{i,a_k} + \sqrt{P}h_i + \mathbf{z}_i^H \mathbf{v}_i, \quad (5)$$

where $h_{i,j} \triangleq \mathbf{z}_i^H \mathbf{H}_{i,j} \mathbf{x}_j$, $h_{i,b_k} \triangleq \mathbf{z}_i^H \mathbf{H}_{i,b_k} \mathbf{x}_{b_k}$, $h_{i,a_k} \triangleq \mathbf{z}_i^H \mathbf{H}_{i,a_k} \mathbf{x}_{a_k}$, and $h_i \triangleq \mathbf{z}_i^H \mathbf{H}_i \mathbf{x}_i$. Then, the performance metric signal-to-interference ratio (SIR) at node i is given by

$$\text{SIR}_i = \frac{L^{-\alpha}|h_{i,j}|^2}{\sum_{k=1}^{M-1}(r_{b_k}^{-\alpha}|h_{i,b_k}|^2 + r_{a_k}^{-\alpha}|h_{i,a_k}|^2) + |h_i|^2}. \quad (6)$$

Here, we ignore the thermal noise effect in SIR due to the assumed interference-limited environment.

III. TRANSCIVER BEAMFORMING DESIGN

In this section, we introduce an efficient transceiver beamforming design to balance desired signal's power and co-channel interference cancellation. With fixed number of transceiver antennas per each node, we formulate the pre-processing/post-processing beamforming vectors at each node to solve the following optimization problem

$$\begin{aligned} & \underset{\mathbf{z}_i, \mathbf{w}_i, \mathbf{w}_{b_k}, \mathbf{w}_{a_k}}{\text{maximize}} && |\mathbf{z}_i^H \mathbf{H}_{i,j} \mathbf{w}_j|^2 \\ & \text{subject to} && |\mathbf{z}_i^H \mathbf{H}_{i,b_k} \mathbf{w}_{b_k}|^2 = 0, \quad k = 1, \dots, l/2, \\ & && |\mathbf{z}_i^H \mathbf{H}_{i,a_k} \mathbf{w}_{a_k}|^2 = 0, \quad k = 1, \dots, l/2, \\ & && |\mathbf{z}_i^H \hat{\mathbf{H}}_i \mathbf{w}_i|^2 = 0, \quad i \neq j \in \{a_0, b_0\}, \end{aligned} \quad (7)$$

where the receiver i aims to cancel the inter-node interference from $l/2$ nearest transceiver pairs. To obtain the optimal

beamforming vector solution, all the nodes need to chase each other's transceiver beams and jointly make the final decision, which is quite challenge and at cost of heavy signalling overhead. This motivates us to design the beamforming vectors in a distributed manner among different transceiver pairs.

By assuming all channel matrices come with full rank, the design criteria follows two conditions: 1) $N_t > N_r$; 2) $N_t \leq N_r$. For the condition that $N_t > N_r$, the SI effect, i.e., $\mathbf{z}_i^H \tilde{\mathbf{H}}_i \mathbf{w}_{i,i \in \{a_0, b_0\}}$, can be nullified by \mathbf{w}_i itself irrespective of \mathbf{z}_i . Then, the node i can spend all its $N_r - 1$ spatial DoFs at receiver side to cancel $\lfloor \frac{N_r-1}{2} \rfloor$ nearest interference pairs. In detail, let's first decompose $\tilde{\mathbf{H}}_i$ into spatial modes by SVD as $\tilde{\mathbf{H}}_i = \mathbf{U}_i \Sigma_i \mathbf{V}_i^H$. Then, the $(\text{rank}(\tilde{\mathbf{H}}_i) + 1)$ to N_t column(s) of \mathbf{V}_i span null space of $\tilde{\mathbf{H}}_i$ and construct a matrix $\tilde{\mathbf{V}}_i$ (or a vector $\tilde{\mathbf{v}}_i$) with size of $N_t \times (\text{rank}(\tilde{\mathbf{H}}_i) + 1 : N_t)$. Then, to improve transmission quality of the desired link, i.e., $\mathbf{H}_{j,i, j \neq i \in \{a_0, b_0\}}$, we need to define $\tilde{\mathbf{H}}_{j,i} \triangleq \mathbf{H}_{j,i} \tilde{\mathbf{V}}_i$, and formulate the SVD of $\tilde{\mathbf{H}}_{j,i}$ as $\tilde{\mathbf{U}}_{j,i} \tilde{\Sigma}_{j,i} \tilde{\mathbf{V}}_{j,i}^H$. Then, the pre-processing beamforming vector at node i can be formulated as

$$\mathbf{w}_i = \tilde{\mathbf{V}}_i \tilde{\mathbf{v}}_{j,i}^{(1)}, \quad i \neq j \in \{a_0, b_0\}, \quad (8)$$

where $\tilde{\mathbf{v}}_{j,i}^{(1)}$ denotes the first column of $\tilde{\mathbf{V}}_{j,i}$. Similar way to formulate pre-processing beamforming vectors for all nodes in Φ_A/a_0 and Φ_B/b_0 . Correspondingly, the post-processing beamforming vector $\mathbf{z}_j, j \neq i \in \{a_0, b_0\}$ at node j can be formulated as

$$\mathbf{z}_j = (\mathbf{s}_j^H \tilde{\mathbf{u}}_{j,i}^{(1)})^{-1} \mathbf{s}_j^H, \quad j \neq i \in \{a_0, b_0\}, \quad (9)$$

where $\tilde{\mathbf{u}}_{j,i}^{(1)}$ denotes the first column of $\tilde{\mathbf{U}}_{j,i}$, and \mathbf{s}_j with size of $N_r \times 1$ is used to span null space of $\mathbf{H}_{j,b_k} \mathbf{w}_{b_k}$ and $\mathbf{H}_{j,a_k} \mathbf{w}_{a_k}$, $k = 1, \dots, l/2$.

For the condition that $N_t \leq N_r$, $\hat{\mathbf{H}}_i$ has full column rank. In this case, we have to cancel the SI plus $\lfloor \frac{N_r-2}{2} \rfloor$ nearest inter-node interference pairs at receiver side. Thus, to improve transmission quality of the desired link, we formulate the pre-processing beamforming vector \mathbf{w}_i at node i as

$$\mathbf{w}_i = \mathbf{v}_{j,i}^{(1)}, \quad i \neq j \in \{a_0, b_0\}, \quad (10)$$

where $\mathbf{v}_{j,i}^{(1)}$ is the first right singular vectors of channel matrix $\mathbf{H}_{j,i}$. Similar way to formulate pre-processing beamforming vectors for all nodes in Φ_A/a_0 and Φ_B/b_0 . Correspondingly, the post-processing beamforming vector $\mathbf{z}_j, j \neq i \in \{a_0, b_0\}$ at node j can be formulated as

$$\mathbf{z}_j = (\mathbf{s}_j^H \mathbf{u}_{j,i}^{(1)})^{-1} \mathbf{s}_j^H, \quad j \neq i \in \{a_0, b_0\}, \quad (11)$$

where $\mathbf{u}_{j,i}^{(1)}$ denotes the first left singular vectors of channel matrix $\mathbf{H}_{j,i}$, and \mathbf{s}_j with size of $N_r \times 1$ in this case is used to span null space of $\hat{\mathbf{H}}_j \mathbf{w}_j$, $\mathbf{H}_{j,b_k} \mathbf{w}_{b_k}$ and $\mathbf{H}_{j,a_k} \mathbf{w}_{a_k}$, $k = 1, \dots, l/2$.

With above discussed transceiver beamforming vectors design, the received signal at typical node $i \neq j \in \{a_0, b_0\}$ can

be expressed as

$$\begin{aligned} \mathbf{z}_i^H \mathbf{y}_i &= \sqrt{P} L^{-\alpha/2} \sqrt{\gamma_{i,j}} s_j + \sqrt{P} \sum_{k=\frac{l}{2}+1}^{M-1} r_{b_k}^{-\alpha/2} h_{i,b_k} \\ &+ \sqrt{P} \sum_{k=\frac{l}{2}+1}^{M-1} r_{a_k}^{-\alpha/2} h_{i,a_k} + \mathbf{z}_i^H \sqrt{P} \Delta_i \mathbf{x}_i, \end{aligned} \quad (12)$$

where $\gamma_{i,j}$ is the largest eigenvalue of $\tilde{\mathbf{H}}_{i,j} \tilde{\mathbf{H}}_{i,j}^H$ for the condition that $N_t > N_r$, and the largest eigenvalue of $\mathbf{H}_{i,j} \mathbf{H}_{i,j}^H$ for the condition that $N_t \leq N_r$. Then, the corresponding SIR can be formulated as

$$\text{SIR}_i = \frac{L^{-\alpha} \gamma_{i,j}}{\sum_{k=\frac{l}{2}+1}^{M-1} r_k^{-\alpha} (|h_{i,b_k}|^2 + |h_{i,a_k}|^2) + |h'_i|^2}, \quad (13)$$

where $h'_i \triangleq \mathbf{z}_i^H \Delta_i \mathbf{x}_i$ is the residual SI effect due to channel estimation error. Here, we assume $r_k \triangleq r_{b_k} = r_{a_k}, \forall k$, where the interference power from each interfering pair is measured from the same distance but with independent channel fading. Such model is widely used to analyse the scaling properties of average sum-rate as in [25], or analyse upper bound of network success probability as in [30].

IV. TRANSMISSION CAPACITY ANALYSIS

There is a probability that high spatial throughput is obtained accompanied with unacceptably high outage, which results in a large number of wasted transmissions. This motivates TC to be proposed to exploit the number of successful transmissions in a unit area with a permissible outage constraint [31]. We assume that the OP, i.e., $q(\lambda)$, is a function of user density λ . Then, the TC formula is given by [31]

$$c(\epsilon) = q^{-1}(\epsilon)(1 - \epsilon)R, \quad \epsilon \in (0, 1), \quad (14)$$

where ϵ is a target OP, and $R = \log_2(1 + \beta)$ is a target transmission rate with SIR threshold β . In general, it is quite difficult to compute the exact closed-form for OP/TC due to the unavailability of closed-form expressions for the distribution of sum of the interferer distances from the typical receiver. This motivates to exploit the closed-form expression of the lower and upper bounds for OP/TC.

A. OP Lower Bound & TC Upper Bound

The OP-LB can be obtained by introducing the dominating interferer pair(s), i.e., the D nearest interferer pair(s) from the typical receiver after the proposed interference cancellation, which is

$$\begin{aligned} q(\epsilon) &= \Pr[\text{SIR}_i < \beta] \\ &> \Pr\left[\frac{1}{\text{SIR}_i^{(d)}} > \frac{1}{\beta}\right], \end{aligned} \quad (15)$$

where

$$\text{SIR}_i^{(d)} \triangleq \frac{L^{-\alpha} \gamma_{i,j}}{\sum_{k=\frac{l}{2}+1}^{\frac{l}{2}+D} r_k^{-\alpha} (|h_{i,b_k}|^2 + |h_{i,a_k}|^2) + |h'_i|^2}$$

²In this paper, we assume the SI always has priority to be cancelled first.

is the SIR consisted of the D dominating interferer pair(s) after the interference cancellation. Here, the dominating interferer pair is defined as its interference contribution alone plus the SI channel estimation error are sufficient to cause outage at the typical receiver. Then, the geometrical location region of the dominating interferer can be obtained as

$$\begin{aligned} R_d &\triangleq \left\{ r_k : \text{SIR}_i^{(1)} = \beta \right\} \\ &= \left[\frac{\beta (|h_{i,b_k}|^2 + |h_{i,a_k}|^2)}{L^{-\alpha} \gamma_{i,j} - \beta |h'_i|^2} \right]^{\frac{1}{\alpha}}, \end{aligned} \quad (16)$$

where R_d is the radius from the typical receiver of the dominating interferer region (e.g. \mathcal{I}). In this case, any node pair after the interference cancellation process located in this region \mathcal{I} is deemed as the dominating interferer pair. Thus, the OP-LB in (15) can be obtained by exploiting its equivalent event that at least one interferer pair is located within the dominating interferer region \mathcal{I} , which is

$$\begin{aligned} q^l(\lambda) &= \Pr \left[r_{\frac{l}{2}+1} \leq R_d \right] \\ &\stackrel{(a)}{=} \mathbb{E}_S \left\{ \mathbb{E}_{SI} \left\{ \frac{\gamma(\frac{l}{2}+1, \lambda \pi \mathbb{E}_\psi \{R_d^2\})}{\Gamma(\frac{l}{2}+1)} \right\} \right\}, \end{aligned} \quad (17)$$

where $\gamma(\cdot, \cdot)$ is the lower incomplete gamma function, $\Gamma(\cdot)$ is the gamma function, $\mathbb{E}_S\{\cdot\}$ is the expectation with respect to (w.r.t.) $\gamma_{i,j}$, $\mathbb{E}_{SI}\{\cdot\}$ is the expectation w.r.t. $|h'_i|^2$, and $\mathbb{E}_\psi\{\cdot\}$ is the expectation w.r.t. $\psi_{i,k} \triangleq |h_{i,b_k}|^2 + |h_{i,a_k}|^2$. In addition, Step (a) in (17) is obtained by formulating the cumulative distribution function of Euclidean distance between the $(\frac{l}{2}+1)^{\text{th}}$ interferer pair and the typical receiver as shown in [32].

To obtain TC-UB, we first need to obtain λ by inverting the OP-LB $q^l(\lambda)$ in (17). However, such operation is infeasible due to the expectation in front of the low incomplete gamma function. On the other hand, with the condition that $a \leq b+1$, $\gamma(a, b)$ is a convex function. In this case, following Jensen's inequality, the OP-LB can be approximated as

$$q^l(\lambda) \approx \frac{\gamma(\frac{l}{2}+1, \lambda \pi \Omega)}{\Gamma(\frac{l}{2}+1)}, \quad (18)$$

where

$$\Omega \triangleq \beta^{\frac{2}{\alpha}} \mathbb{E}\{\psi_{i,k}^{\frac{2}{\alpha}}\} \left(\frac{\mathbb{E}\{\gamma_{i,j}\}}{L^\alpha} - \beta \mathbb{E}\{|h'_i|^2\} \right)^{-\frac{2}{\alpha}}. \quad (19)$$

Here, we should have $\frac{l}{2} \leq \lambda \pi \Omega$. Then, following Taylor expansion of the lower incomplete Gamma function as in [33], (18) can be converted to

$$q^l(\lambda) = \frac{(\pi \Omega)^{\frac{l}{2}+1}}{\Gamma(\frac{l}{2}+1)} \sum_{m=0}^{\infty} \frac{(-\pi \Omega)^m}{m!} \frac{\lambda^{m+\frac{l}{2}+1}}{m+\frac{l}{2}+1}. \quad (20)$$

Then, to find λ such that $q^l(\lambda) = \epsilon$, we can resort to Newton-Raphson method [34]. Specifically, let's start from an initial guess λ_0 for a root of the function $q^l(\lambda) = \epsilon$, which is

$$\lambda_0 = \frac{1}{\pi \Omega} \left(\epsilon \Gamma(\frac{l}{2}+1) \Gamma(\frac{l}{2}+1) \right)^{\frac{1}{\frac{l}{2}+1}}, \quad (21)$$

where (21) is formulated by solving $\lambda_0 : q^l(\lambda_0) = \epsilon$ with a single term in (20). To refine this approximation, we have

$$\lambda_1 = \lambda_0 - \frac{q^l(\lambda_0)}{q'^l(\lambda_0)}, \quad (22)$$

where $q'^l(\lambda_0)$ is the first order derivative of $q^l(\lambda_0)$. Consequently, this should give

$$\begin{aligned} \lambda_{n+1} &= \lambda_n + \lambda_n e^{\lambda_n \pi \Omega} (\lambda_n \pi \Omega)^{-\frac{l}{2}-1} \\ &\quad \cdot \left(\Gamma(\frac{l}{2}+1, \lambda_n \pi \Omega) + (\epsilon - 1) \Gamma(\frac{l}{2}+1) \right), \end{aligned} \quad (23)$$

where $\Gamma(a, b)$ is the upper incomplete gamma function. Then, following the TC formula in (14), we have

$$c^u(\epsilon) = \lambda_{n+1} (1 - \epsilon) R. \quad (24)$$

It is worth noting that several iterations in general will lead to a sufficiently accurate value of λ .

B. Distribution Analysis of Random Variables

In order to obtain the explicit expressions for OP-LB and TC-UB, we need to find the expected values of the random variables involved in (18) and (24). Start from the distribution of $|h'_i|^2$. Since the SI channel estimation error Δ_i follows i.i.d. complex Gaussian distribution with zero mean and $\sigma_{i,\text{SI}}^2/2$ variance per element, and the multiplied pre-processing/post-processing beamforming vectors are independent of Δ_i , following the proof in [20], we have $h'_i \sim \mathcal{CN}(0, \sigma_{i,\text{SI}}^2/2)$ and $|h'_i|^2 \sim \Gamma(1, \sigma_{i,\text{SI}}^2)$. Similarly, we have $|h_{i,b_k}|^2 \sim \text{Exp}(1)$ and $|h_{i,a_k}|^2 \sim \text{Exp}(1)$, so that $\psi_{i,k} \sim \Gamma(2, 1)$ and $\psi_{i,k}^{2/\alpha}$ follows a generalized gamma distribution with parameters $(1, \alpha, \alpha/2)$. Thus, we have $\mathbb{E}\{|h'_i|^2\} = \sigma_{i,\text{SI}}^2$, $\mathbb{E}\{\psi_{i,k}\} = 2$, and $\mathbb{E}\{\psi_{i,k}^{\alpha/2}\} = \Gamma(2 + 2/\alpha)/2$.

For the desired signal, the explicit distribution of the largest eigenvalue $\gamma_{i,j}$ in general is difficult to find. However, if the eigenvalue $\gamma_{i,j}$ is obtained from a Wishart matrix, based on [35], we can find its distribution from the upper and the lower bound values of $\gamma_{i,j}$. Specifically, for the condition that $N_t \leq N_r$, $\gamma_{i,j}$ is obtained directly from $\mathbf{H}_{i,j} \mathbf{H}_{i,j}^H$, where $\mathbf{H}_{i,j} \mathbf{H}_{i,j}^H$ is a Wishart matrix due to complex Gaussian distribution on $\mathbf{H}_{i,j}$; For the condition that $N_t > N_r$, we have

$$\begin{aligned} \tilde{\mathbf{H}}_{i,j} \tilde{\mathbf{H}}_{i,j}^H &= \mathbf{H}_{i,j} \tilde{\mathbf{V}}_j \tilde{\mathbf{V}}_j^H \mathbf{H}_{i,j}^H \\ &\stackrel{(a)}{=} \mathbf{H}_{i,j} \mathbf{T}_j \mathbf{\Lambda}_j \mathbf{T}_j^H \mathbf{H}_{i,j}^H, \end{aligned} \quad (25)$$

where $\tilde{\mathbf{V}}_j$ is formulated from the estimated SI channel $\hat{\mathbf{H}}_j$ similar as the way to formulate $\tilde{\mathbf{V}}_i$ in Sec. III. In addition, Step (a) in (25) is obtained by applying the eigenvalue decomposition to $\tilde{\mathbf{V}}_j \tilde{\mathbf{V}}_j^H$, where $\mathbf{\Lambda}_j = \text{diag}(\underbrace{[1, \dots, 1, 0, \dots, 0]}_{N_t - N_r}, \underbrace{}_{N_r})$, and \mathbf{T}_j is

a $N_t \times N_t$ unitary matrix whose columns are the eigenvectors of $\tilde{\mathbf{V}}_j \tilde{\mathbf{V}}_j^H$. Then, by applying the unitary invariance property on $\mathbf{H}_{i,j}$, we obtain that $\tilde{\mathbf{H}}_{i,j} \tilde{\mathbf{H}}_{i,j}^H$ is also a Wishart matrix regardless the distribution on the estimated SI channel $\hat{\mathbf{H}}_j$.

Consequently, the largest eigenvalue $\gamma_{i,j}$ of $\mathbf{H}_{i,j}\mathbf{H}_{i,j}^H$ is bounded by [35]:

$$\|\mathbf{H}_{i,j}\|^2 \geq \gamma_{i,j} \geq \frac{\|\mathbf{H}_{i,j}\|^2}{N_t}, \quad (26)$$

where $\|\mathbf{H}_{i,j}\|^2$ follows χ^2 distribution with $2N_tN_r$ degrees of freedom. Then, $\mathbb{E}\{\gamma_{i,j}\}$ can be lower bounded by $\mathbb{E}\{\|\mathbf{H}_{i,j}\|^2/N_t\} = 2N_r$. Similarly, the largest eigenvalue $\gamma_{i,j}$ of $\tilde{\mathbf{H}}_{i,j}\tilde{\mathbf{H}}_{i,j}^H$ is bounded by [35]:

$$\|\tilde{\mathbf{H}}_{i,j}\|^2 \geq \gamma_{i,j} \geq \frac{\|\tilde{\mathbf{H}}_{i,j}\|^2}{N_r}, \quad (27)$$

where $\|\tilde{\mathbf{H}}_{i,j}\|^2$ follows χ^2 distribution with $2N_r(N_t - N_r)$ degrees of freedom. Then, $\mathbb{E}\{\gamma_{i,j}\}$ can be lower bounded by $\mathbb{E}\{\|\tilde{\mathbf{H}}_{i,j}\|^2/N_r\} = 2(N_t - N_r)$. By inserting the obtained $\mathbb{E}\{|h_i|^2\}$, $\mathbb{E}\{\psi_{i,k}^{\alpha/2}\}$ and the lower bound of $\mathbb{E}\{\gamma_{i,j}\}$ back into (18) and (24), we obtain the explicit OP-LB and TC-UB.

C. TC Upper Bound of HD Case

For comparison, we provide TC-UB of HD case. Unlike TC-UB of FD case, there is only one transmit node per transceiver pair in HD case, where the locations of the transmit nodes form Poisson distribution with intensity λ . Since, there is no SI effect, the pre-processing beamforming vector per transmitter will be the first right singular vector of the corresponding direct link's channel matrix, e.g., as in (10). Meanwhile, the post-processing beamforming vector per receiver will be formulated following the way as in (11).

To obtain the TC-UB of HD case, we first derive its OP-LB by defining the geometrical location region of its dominating interferer as

$$R_d^{\text{HD}} = \left[\frac{\beta |h_{i,b_{l+1}}|^2}{L^{-\alpha} \gamma_{i,j}} \right]^{\frac{1}{\alpha}}, \quad (28)$$

where (28) is formulated similar as (16) but has removed effects from node a_{l+1} and SI. Then, the corresponding OP-LB can be obtained by replacing R_d in (17) with R_d^{HD} in (28), and its approximation is given by

$$q^{l,\text{HD}}(\lambda^{\text{HD}}) \approx \frac{\gamma(l, \lambda^{\text{HD}} \pi \Omega^{\text{HD}})}{\Gamma(l+1)}, \quad (29)$$

where λ^{HD} is the network intensity of HD case, and

$$\Omega^{\text{HD}} \triangleq \beta^{\frac{2}{\alpha}} \mathbb{E}\{|h_{i,b_k}|^{\frac{4}{\alpha}}\} \left(\frac{\mathbb{E}\{\gamma_{i,j}\}}{L^\alpha} \right)^{-\frac{2}{\alpha}}. \quad (30)$$

Then, the network intensity λ^{HD} can be formulated by following (20) to (23). Finally, the TC-UB of HD case can be obtained as

$$c^{u,\text{HD}}(\epsilon) = 2\lambda_{n+1}^{\text{HD}}(1 - \epsilon)R. \quad (31)$$

Here, to remove the expectations in HD TC-UB formula, we calculate $\mathbb{E}\{|h_{i,b_k}|^{\frac{4}{\alpha}}\} = \Gamma(1 + 2/\alpha)$ and $\mathbb{E}\{\gamma_{i,j}\}$ follows (25).

V. SIMULATION AND NUMERICAL RESULTS

In this section, we provide several simulation and numerical examples to exam the accuracy of our derived TC-UB and compare the proposed beamforming design with some existing

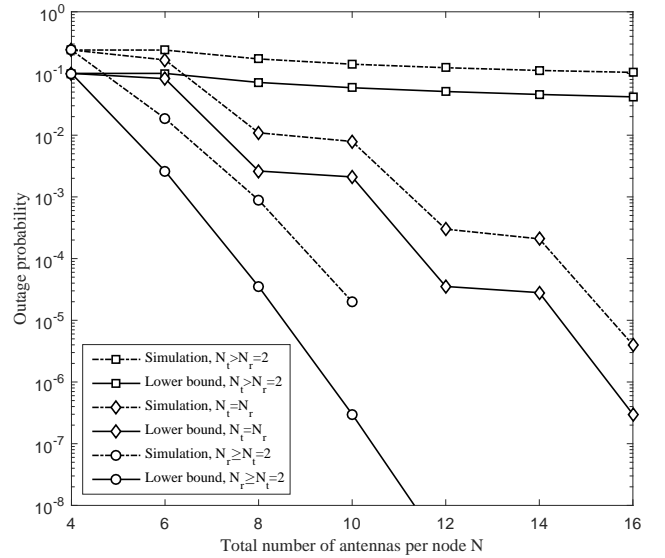


Fig. 2: Outage probability versus the total number of antennas per node, where $L = 1$, $P = 1$, $\alpha = 4$, $\lambda = 0.1$, $\sigma_{i,\text{SI}}^2 = 0.1$, and $\beta = 1$.

methods, e.g., SVD based method as in [19]; SVD plus partial ZF based method as in [20], and purely partial ZF based method as in [21]. Here, all these three existing methods utilize one of their receiver DoFs to cancel the SI effect. In addition, we also compare our derived TC-UB of FD case with the TC-UB of HD case. We assume that the simulated FD MIMO ad-hoc network lies on a 2-D disk with a number of transceiver pairs, where their locations follow Poisson random variable with its mean equal to 200. All the channels except SI channel are with $\alpha = 4$ free pass loss exponent and follow independent Rayleigh distribution.

Experiment 1: In this experiment, we test the derived OP-LB and TC-UB by comparing with the corresponding simulation results. As shown in Fig. (2), our derived OP-LB is quite close to the simulation result for different TRR configurations. However, accompanied with number of receive-antenna increasing, the performance gap is increased as well. This is due to the increased number of cancelled inter-node interference. The more inter-node interferences being cancelled, the smaller probability that at least one interferer pair is located within the dominating interferer region. On the other hand, the simulated curve shows performance with all accumulated non-dominating interferers in the network. Similar performance trend can be observed for TC-UB in Fig. (3). The kinked curves for the case that $N_t = N_r$ are purely due to the specified transceiver antenna configuration.

Experiment 2: In this experiment, we compare the proposed beamforming design method with the above mentioned three existing methods. As shown in Fig. 4, the proposed beamforming design outperforms the SVD plus partial ZF method when the total number of antenna per node is greater than 12. This is because our proposed method takes the advantage of

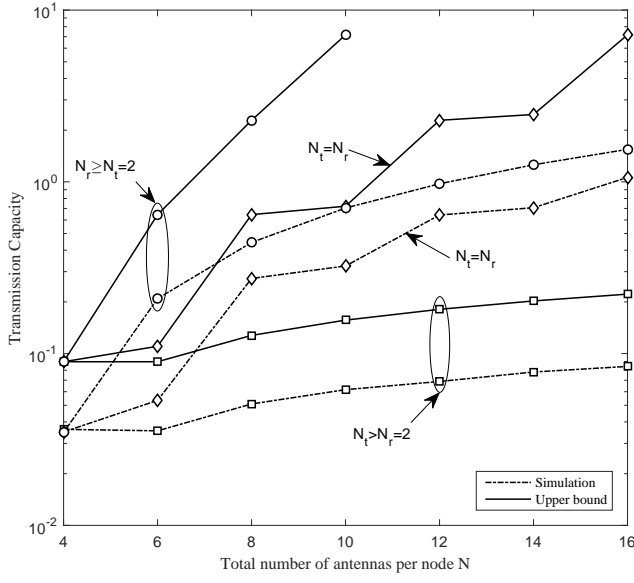


Fig. 3: Transmission Capacity versus the total number of antennas per node, where $L = 1$, $P = 1$, $\alpha = 4$, $\epsilon = 0.1$, $\sigma_{i,SI}^2 = 0.1$, and $\beta = 1$.

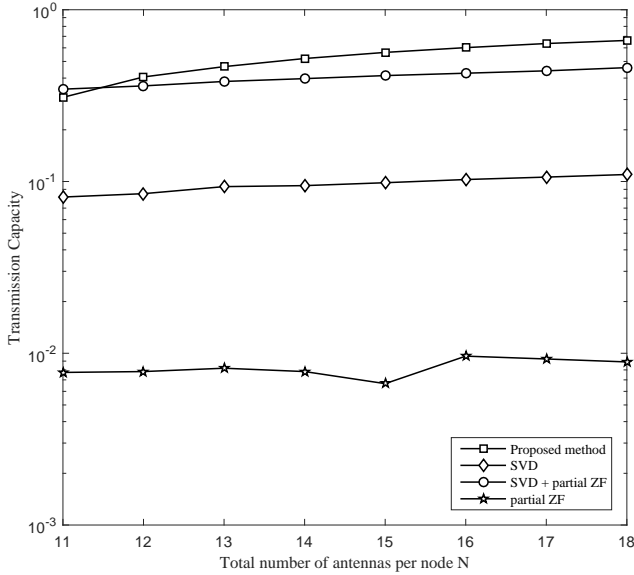


Fig. 4: Transmission Capacity versus the total number of antennas per node in comparison among different beamforming methods, where $L = 1$, $P = 1$, $\alpha = 4$, $\epsilon = 0.1$, $\sigma_{i,SI}^2 = 0.1$, $\beta = 1$, and $N_r = 5$.

the specified TRR configuration, i.e., $N_t > N_r$. In this case, SI can be cancelled at the transmitter side, and it will leave an additional DoF at receiver side for inter-node interference cancellation. However, when $N = 11$, the proposed method shows a worse performance by comparing with SVD plus partial ZF method. This is because in this case only one DoF is left at the transmitter side and has been used for SI

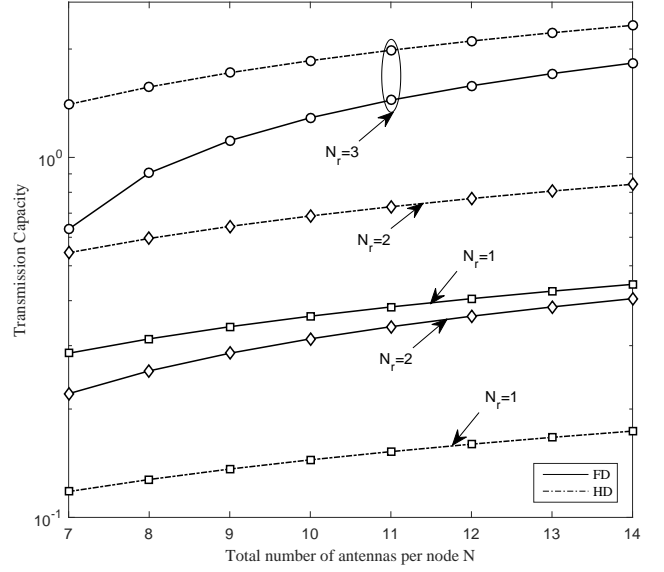


Fig. 5: Transmission Capacity versus the total number of antennas per node in comparison between FD case and HD case, where $L = 1$, $P = 1$, $\alpha = 4$, $\epsilon = 0.1$, $\sigma_{i,SI}^2 = 0.1$, and $\beta = 1$.

cancellation. In contrast, the SVD plus partial ZF method is able to use that DoF at transmitter side to boost its the desired channel link, and leave the SI to be cancelled at receiver side. In addition, the proposed scheme outperforms another two methods throughout the entire N range.

Experiment 3: In this experiment, we compare our derived TC-UB of FD case with TC-UB of HD case. As shown in Fig. 5, the TC-UB of FD case outperforms the TC-UB of HD case when $N_r = 1$. If we increase the number of receive-antenna, more dominating (or nearest) interferers can be cancelled. In this case, the TC-UB of HD case outperforms the TC-UB of FD case. This indicates more dominating interferers with different locations can be cancelled in HD case. However, although FD can double the rate, the dominating interferer pair at the same location in FD case will limit its capability to cancel dominating interferers with different locations. In other words, after the interference cancellation, more interferers are existing in the dominating interferer region in FD case. This motivates us to continue this work to exploit the benefit of adaptive FD MIMO communications.

VI. CONCLUSION

In this paper, we have proposed a joint transceiver beamforming design for FD MIMO ad-hoc network to mitigate inter-node interference and partial SI in spatial domain. The TC-UB of the considered network has been derived at present of SI channel estimation error. Computer simulations have been conduct to show that the derived TC-UB is quite close to the actual one especially when the number of receive-antenna is small, and the proposed beamforming design outperforms the existing beamforming methods when the TRR greater than

one. In addition, we also compared the TC-UB of FD case with the ones of HD case, and the result indicates the importance of dominating interference cancellation capability.

ACKNOWLEDGEMENT

This work was supported by the Engineering and Physical Science Research Council (EPSRC) through the Scalable Full Duplex Dense Wireless Networks (SENSE) grant EP/P003486/1.

REFERENCES

- [1] I. Orikumhi, C. Y. Leow, and Z. Ding, "Wireless information and power transfer in MIMO virtual full-duplex relaying system," *IEEE Trans. Veh. Technol.*, pp. 1–10, 2017.
- [2] N. Anjum, D. Karamshuk, M. Shikh-Bahaei, and N. Sastry, "Survey on peer-assisted content delivery networks," *Computer Networks*, vol. 116, pp. 79–95, Apr. 2017.
- [3] K. Nehra, A. Shadmand, and M. Shikh-Bahaei, "Cross-layer design for interference-limited spectrum sharing systems," in *Proc. IEEE Global Telecommunications Conf.*, Dec. 2010, pp. 1–5.
- [4] V. Towhidlou and M. Shikh-Bahaei, "Improved cognitive networking through full duplex cooperative arq and harq," *IEEE Wireless Commun. Lett.*, vol. 7, pp. 218–221, Apr. 2018.
- [5] A. Sabharwal, P. Schniter, D. Guo, D. W. Bliss, S. Rangarajan, and R. Wichman, "In-band full-duplex wireless: Challenges and opportunities," *IEEE J. Sel. Areas Commun.*, vol. 32, no. 9, pp. 1637–1652, Sept. 2014.
- [6] D. Kim, H. Lee, and D. Hong, "A survey of in-band full-duplex transmission: From the perspective of phy and mac layers," *IEEE Commun. Surv. Tutor.*, vol. 17, no. 4, pp. 2017–2046, 2015.
- [7] V. Towhidlou and M. Shikh-Bahaei, "Cooperative ARQ in full duplex cognitive radio networks," in *Proc. IEEE Int. Symp. Personal, Indoor and Mobile Radio Communications*, Dec. 2016, pp. 1–5.
- [8] M. Naslcheraghi, S. A. Ghorashi, and M. Shikh-Bahaei, "FD device-to-device communication for wireless video distribution," *IET Commun.*, vol. 11, no. 7, pp. 1074–1081, May 2017.
- [9] J. I. Choi, M. Jain, K. Srinivasan, P. Levis, and S. Katti, "Achieving single channel, full duplex wireless communications," in *Proc. ACM MobiCom*, 2010, pp. 1–12.
- [10] E. Everett, A. Sahai, and A. Sabharwal, "Passive self-interference suppression for full-duplex infrastructure nodes," *IEEE Trans. Wireless Commun.*, vol. 13, no. 2, pp. 680–694, Feb. 2014.
- [11] M. Duarte and A. Sabharwal, "Full-duplex wireless communications using off-the-shelf radios: feasibility and first results," in *Proc. 44th Asilomar Conf. Signals Syst. Comput.*, Nov. 2010, pp. 1558–1562.
- [12] M. e. a. Jain, "Practical, real-time, full duplex wireless," in *Proc. ACM MobiCom*, Sept. 2011, pp. 301–313.
- [13] M. Duarte, C. Dick, and A. Sabharwal, "Experiment-driven characterization of full-duplex wireless systems," *IEEE Trans. Wireless Commun.*, vol. 11, no. 12, pp. 4296–4307, Dec. 2012.
- [14] A. Olfat and M. Shikh-Bahaei, "Optimum power and rate adaptation with imperfect channel estimation for mqam in rayleigh flat fading channel," in *Proc. IEEE Veh. Tech. Conf.*, Sept. 2005, pp. 2468–2471.
- [15] A. Shadmand, K. Nehra, and M. Shikh-Bahaei, "Cross-layer design in dynamic spectrum sharing systems," *EURASIP Journal on Wireless Communications and Networking*, vol. 2010, pp. 1–8, Dec. 2010.
- [16] M. M. Mahyari, A. Shojaeifard, and M. Shikh-Bahaei, "Probabilistic radio resource allocation over cdma-based cognitive radio networks," *IEEE Trans. Veh. Technol.*, vol. 64, no. 8, pp. 3560–3565, Aug. 2015.
- [17] Y. Huang, G. Zheng, M. Bengtsson, K. Wong, L. Yang, and B. Ottersten, "Distributed multicell beamforming with limited intercell coordination," *IEEE Trans. Signal Process.*, vol. 59, no. 2, pp. 728–738, Feb. 2011.
- [18] J. Hou, N. Yi, and Y. Ma, "Joint space-frequency user scheduling for MIMO random beamforming with limited feedback," *IEEE Trans. Commun.*, vol. 63, no. 6, pp. 2224–2236, Jun. 2015.
- [19] A. M. Hunter, J. G. Andrews, and S. Weber, "Transmission capacity of ad hoc networks with spatial diversity," *IEEE Trans. Wireless Commun.*, vol. 7, no. 12, pp. 5058–5071, Dec. 2008.
- [20] R. Vaze and R. W. Heath, "Transmission capacity of ad-hoc networks with multiple antennas using transmit stream adaptation and interference cancellation," *IEEE Trans. Inf. Theory*, vol. 58, no. 2, pp. 780–792, Feb. 2012.
- [21] K. Huang, J. G. Andrews, D. Guo, R. W. Heath, Jr., and R. A. Berry, "Spatial interference cancellation for multiantenna mobile ad hoc networks," *IEEE Trans. Inf. Theory*, vol. 58, no. 3, pp. 1660–1676, Mar. 2012.
- [22] T. Riihonen, S. Werner, and R. Wichman, "Mitigation of loopback self-interference in full-duplex MIMO relay," *IEEE Trans. Signal Process.*, vol. 59, no. 12, pp. 5983–5993, Dec. 2011.
- [23] D. Senaratne and C. Tellambura, "Beamforming for space division duplex," in *Proc. IEEE Int. Conf. Communications*, Jun. 2011, pp. 1–5.
- [24] S. Huberman and T. Le-Ngoc, "MIMO full-duplex precoding: a joint beamforming and self-interference cancellation structure," *IEEE Trans. Wireless Commun.*, vol. 14, no. 4, pp. 2205–2217, Apr. 2015.
- [25] H. Ju, D. Kim, H. V. Poor, and D. Hong, "Bi-directional beamforming and its capacity scaling in pairwise two-way communications," *IEEE Trans. Wireless Commun.*, vol. 11, no. 1, Jan. 2012.
- [26] R. K. Mungara, I. Thibault, and A. Lozano, "Full-duplex MIMO in cellular networks: System-level performance," *IEEE Trans. Wireless Commun.*, vol. 16, no. 5, pp. 3124–3137, May 2017.
- [27] I. Atzeni and M. Kountouris, "Full-duplex mimo small-cell networks with interference cancellation," *IEEE Trans. Wireless Commun.*, vol. 16, no. 12, pp. 8362–8376, Dec. 2017.
- [28] N. Jindal, J. G. Andrews, and S. Weber, "Multi-antenna communication in ad hoc networks: Achieving MIMO gains with SIMO transmission," *IEEE Trans. Commun.*, vol. 59, no. 2, pp. 529–540, Feb. 2011.
- [29] M. Haenggi, *Stochastic Geometry for wireless Networks*. Cambridge, U.K.: Cambridge university Press, 2012.
- [30] Z. Tong and M. Haenggi, "Throughput analysis for full-duplex wireless networks with imperfect self-interference cancellation," *IEEE Trans. Commun.*, vol. 63, no. 11, pp. 4490–4500, Nov. 2015.
- [31] S. Weber, J. G. Andrews, and N. Jindal, "An overview of the transmission capacity of wireless networks," *IEEE Trans. Commun.*, vol. 58, no. 12, pp. 3593–3604, Dec. 2010.
- [32] M. Haenggi, "On distances in uniformly random networks," *IEEE Trans. Inf. Theory*, vol. 51, no. 10, pp. 3584–3586, Oct. 2005.
- [33] M. A. and I. Stegun, *Handbook of Mathematical Functions with Formulas, Graphs, and Mathematical Tables*. New York: Dover Publications Inc., 1970.
- [34] E. Suli and D. Mayers, *An Introduction to Numerical Analysis*, 1st ed. Cambridge, UK: Cambridge University Press, Sept. 2003.
- [35] R. A. Horn and C. R. Johnson, *Matrix Analysis*. Cambridge, United Kingdom: Cambridge University Press, 1985.